Security level classification based on power system partitioning

Zhigang Lu[a],[*] Boxuan Zhao[b], Liangce He[a], Dan Zhang[c], Jiangfeng Zhang[d]

[a]Key Lab of Power Electronics for Energy Conservation and Motor Drive of Hebei Province, Yanshan University, Qinhuangdao, Hebei, 066004, China
[b]Beijing Kedong Electric Power Control System Co., Ltd, Beijing 100192
[c]Handan Weixian Power Supply Company, Weixian, Hebei, 056800, China
[d]School of Electrical and Data Engineering, University of Technology Sydney, Sydney, Australia
*zhglu@ysu.edu.cn

Abstract: Secure and reliable operation of power systems is a crucial factor to the security of power supply, and security assessment is an effective way to evaluate the quality of security. In order to evaluate the specific security status of a power system, a novel method for security level classification (SLC) based on power system partitioning is proposed in this paper. In this method, power system is partitioned into different subareas satisfying different *N-k* contingencies. Then the mutual power supply between each subarea is coordinated to obtain the total supply capacity (TSC) under *N-k* contingencies.The security margin index (SM), average system disequilibrium index (ASD) and comprehensive safety index (CSI) are applied to assess the security of power system. Besides this, the threshold crossing index (TC) and the loss rate of load index (LRL) are applied to assess the unsafe conditions of power systems. According to the above procedures, the power system security states are classified into 5 levels, and a quantitative criterion to determine the exact security level is also given. Finally, a practical power system and the IEEE 118-bus test system are adopted to validate the feasibility of security classification based on *N-k* contingencies partition.

Key words: security level classification (SLC); power system partitioning; *N-k* contingencies; security indexes; total supply capacity (TSC)

1. Introduction

With the development of economy and the continuous urbanization, electricity consumption is increasing rapidly in many countries. The relationship between economy and power supply is quite close [1], and any shortage of power supply or power outage accident will bring huge economic losses. Therefore, security and reliability of power supply are extremely important to economic development [2], and it is necessary to assess the security of power system, and find out the weakness of the power system so as to take further actions to strengthen the security of power supply.

Traditional security assessment of power systems mainly focuses on one aspect of the operation state or power system structure, and these two factors have not been successfully combined in existing studies. The impact of constraints on power system operational security is studied in [3]. The operation risk of power system is considered in [4, 5]. Note that these studies in [3-5] do not consider the influence of power system structure, then topological structure security of power system is studied in [6]. The security of the power equipment in power system is investigated in [7]. However, these studies do not consider the impact of operation status.

With the increase of power consumption, the scale of regional power systems keeps on increasing, which brings a huge challenge to guarantee the security of power systems [8, 9]. Besides this, it may cause the "dimension disaster" due to the enormous amount of calculation [10]. In [11], a method of fast *N-k* contingencies for power system is proposed, which significantly improves the speed of *N-k* contingencies computation. Most of the traditional security assessments of power systems evaluates the overall power system [12, 13], and focusing on the comparison of the different power systems. This kind of system wide assessment method cannot intuitively identify the specific weakness of the power system. Therefore, it is necessary to partition the power system, and then assess their security for each subarea. There are many methods of power system partitioning. In [14, 15], the power system is partitioned by considering reactive voltage coupling relationship among the nodes of power system. In [16, 17], the power system is partitioned based on PMU measurements ares, the method segregated a power system into different areas which can be effectively used for vulnerability assessment. In [18], the power system is partitioned according to the area ownership of the power system, but it splits the electrical connections of the subareas.

Based on the above viewpoints and previous studies, this paper proposes a new method of security level classification based on power system partitioning. In order to consider the operation and the power system structure at the same time, the partitioning method is based on different *N-k* contingencies. The method will assess security by calculating the total supply capacity (TSC), and it fully reflects the security of power system structure and the differences of the structures among different subareas. TSC is an important index to reflect the power supply capability, and TSC is usually solved by DC power flow algorithms [19] or AC power flow algorithms [20]. DC power flow algorithm is fast, but the precision is poor. The AC power flow algorithm has high accuracy, while the speed is slow. In order to compute the TSC considering both the

computational accuracy and speed, the TSC is obtained through the cone programming method. This paper establishes a comprehensive security assessment method to classify the security level of each subarea of the power system.

Key contributions of this paper are highlighted below:

1)The proposed security level classification based on power system partitioning can reflect the operation status and system structure of the power system.

2)The proposed power system partitioning method is based on *N-k* contingencies. Power system is divided into several subareas according to the proposed partitioning method, and isolated nodes are merged into the nearby subareas according to the coupling relationship among nodes.

3)The security level of each subarea power system is obtained according to the comprehensive safety index (CSI), and the CSI considers the influence of system disequilibrium degree and safety load margin. In order to reflect accidents, this paper applies the loss rate of load (LRL) to reflect the severity of the load loss, and threshold crossing index (TC) to reflect the risk of exceeding the limits.

The rest of this paper is organized as follows. The partitioning method of power system is introduced in section 2. The TSC model and its computing method are given in section 3. The security indexes are presented in section 4. The security levels classification of power system method is introduced in section 5. The conclusions are drawn in the end.

2. Partitioning method of power system

Since the scale of power system keeps on increasing, the calculation of power system may cause "dimension disaster". One of the methods to avoid "dimension disaster" is the power system partitioning, which can reduce the computational complexity by calculating each subarea separately. The security of power systems depends on both the structures and operation status, and the *N-k* contingencies take full account of the two factors. Therefore, the power system is partitioned into several subareas according to the *N-k* contingencies.

For practical power systems, few of them can withstand *N*-3 contingencies. Therefore, *N*-1 contingency, *N*-2 contingencies, and *N*-3 contingencies are mainly considered for the *N-k* contingencies in this paper.

The general partitioning method can be illustrated by considering an example to partition a power system into 4 types A, B, C, D which can defend *N*-3 contingencies. The types A, B, and C can defend *N*-3, *N*-2, *N*-1 contingency, respectively. Type D cannot withstand *N*-1 contingencies.

Specific partitioning steps are as follows:

1) The transmission lines are divided into input lines, output lines, and tie-lines. The input lines are the transmission lines which supply power to the substations. The output lines are the lines which connect to the power output side of substations. The tie-lines are the line connecting different areas which allow bidirectional power flow.

2) A rough partition on the power system is based on its structure. Subarea A can reach any substation with at least four input lines or tie-lines. Subarea B can reach any substation with at least three input lines or tie-lines. Subarea C can reach any substation with at least two input lines or tie-lines. The power system structure of subarea D does not have the above requirement on the number of input or tie-lines.

3) The load is considered on the basis of the power system structure. Under the maximum load, all the substations and lines of a sub-area cannot violate their constraints in *N-k* contingencies. Otherwise, the *N-k*+1 contingencies are carried out, until the power system of this subarea cannot defend *N*-1 contingency.

4) After partitioning some isolated nodes may be left, the isolated nodes will be incorporated into a nearby subarea according to the coupling degree among the nodes [21], and then the final partitioning results are obtained.

5) If a certain area fails, there will be no instability in other regional power grids.

Schematic diagram of sub-areas connection is shown as Fig. 1.

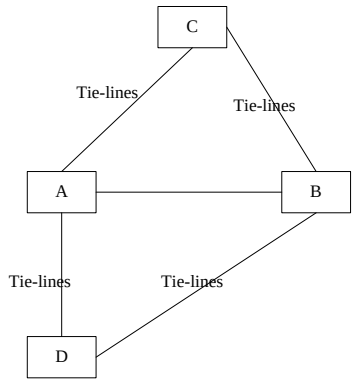

Fig. 1 Schematic diagram of subarea connection

The flow chart of partitioning is shown as Fig. 2.

3. Model of total supply capacity based on cone programming

3.1. Contingencies screening based on total maximum network flow

Because usually there are too many electrical elements in a power system, contingency analysis needs to be repeated many times. In order to improve the calculation efficiency, one of the methods is to screen and analyze the contingencies [22]. In this paper, the maximum network flow method is used to screen the contingencies which have greater influence on TSC [23].The system performance index (SPI) is defined as follows:

$$\begin{cases} SPI_i = \dfrac{E_0^{\max} - E_i^{\max}}{E_0^{\max}} \\ E_0^{\max} = \sum_{g\in Gl\in L}\sum P_{(g.l)}^{\max} \\ P_{(g.l)}^{\max} = \varphi(A,C) \end{cases} \tag{1}$$

In the above formula, $E_0^{\max}$ indicates the maximum network flow under normal operation of power system, $E_{\mathrm{i}}^{\max}$ is the maximum network flow under the contingency *i*, φ is the network maximum flow computation function, *A* is the topological matrix of the power system, *C* is the capacity

matrix of transmission lines, and $P_{(g,l)}^{\max}$ represents the maximum transmission power of the generator node to the load node.

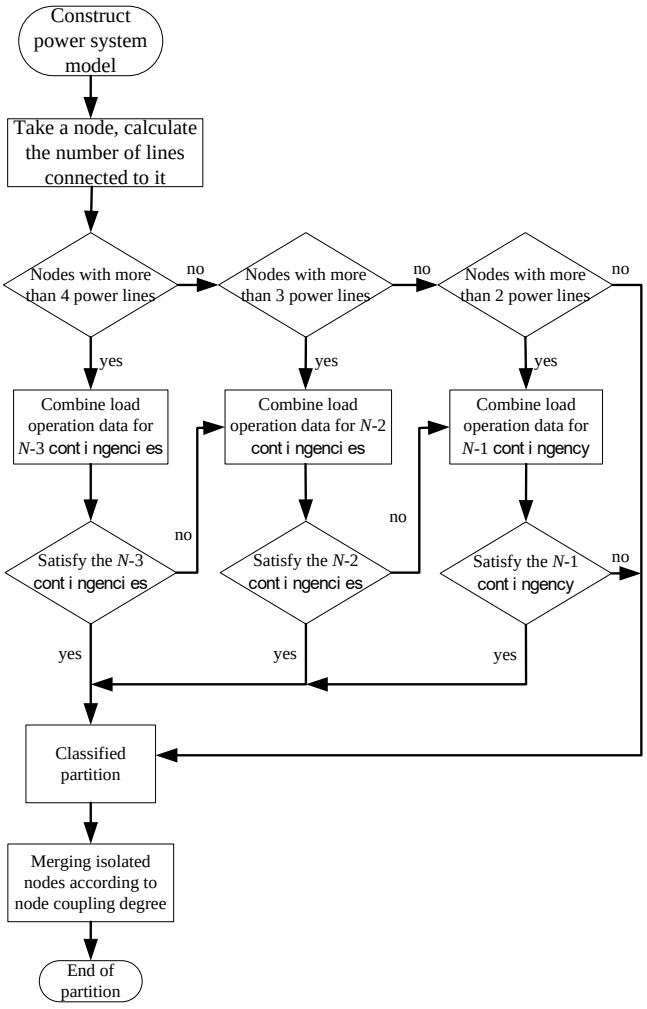

Fig. 2 Flow chart of Partitioning

3.2. Model of total supply capacity

Total supply capacity is the maximum load supply capacity under the security operation constraints [24]. In order to obtain the security level of power systems under *N-k* contingencies, this paper calculates the TSC value under the *N-k* contingencies.

1) Objective function

$$TSC = \max \sum_{i=1}^{n} \left| P_i \right| \tag{2}$$

where P_i is the load of node *i* and *n* is the number of load nodes.

2) Constraints

Power flow constraints

$$\begin{cases} P_{i\min} \le P_i \le P_{imax} \\ Q_{i\min} \le Q_i \le Q_{imax} \\ P_i = G_{ii} V_{\mathrm{i}}^2 + \sum_{j \in N(i)} V_i V_j \left(G_{ij} \cos\theta_{ij} + B_{ij} \sin\theta_{ij} \right) \\ Q_i = -B_{ii} V_{\mathrm{i}}^2 + \sum_{j \in N(i)} V_i V_j \left(B_{ij} \cos\theta_{ij} - G_{ij} \sin\theta_{ij} \right) \end{cases} \tag{3}$$

Voltage magnitude limits

$$V_{i\min} \le V_i \le V_{i\max} \tag{4}$$

Lines current constraints

$$I_{ij}^{\ 2} = a_{ij} V_i^2 + b_{ij} V_j^{\ 2} - 2 V_i V_j (c_{ij} \cos\theta_{ij} - d_{ij} \cos\theta_{ij}) \le I_{ij\max}^{\ 2} \tag{5}$$

where $a_{ij} = g_{ij} + (b_{ij} + b_{shij})$, $b_{ij} = g_{ij}^{\ 2} + b_{ij}^{\ 2}$, $c_{ij} = g_{ij}^{\ 2} + b_{ij}(b_{ij} + b_{shij}/2)$, $d_{ij} = g_{ij} b_{shij}/2$, g_{ij} and b_{ij} are the series conductance and susceptance in the π equivalent model and $b_{shij}/2$ is the 1/2 charging susceptance in accordance with line *ij*. G_{ii} is the self-conductance in the node admittance matrix. B_{ii} is self-susceptance, G_{ij} is the mutual conductivity, B_{ij} is the mutual conductivity, B_{ij} is the mutual susceptance. V_i , V_j and θ_{ij} are the voltage magnitude of node *i*, *j* and the voltage angle difference between nodes *i* and *j*, respectively. $P_{imax,}$ P_{imin} are the active power maximum limit and minimum limit of node *i*, respectively. Q_{imax}, Q_{imin} are the reactive power maximum limit and minimum limit of node *i*, respectively. $V_{i\max}$, $V_{i\min}$ are the maximum voltage limit and the minimum voltage limit of node *i*, respectively. I_{ij} , $I_{ij\max}$ are the magnitude of the branch current and its maximum limit, respectively.

Cone programming method has been successfully applied to the network reconfiguration and operation of traditional distribution networks [25]. This method can solve the optimization problem quickly and accurately, but this method has strict requirements for the mathematical model of optimization problem. Therefore, the above TSC model is converted into cone model according to the standard form of cone programming method [26]. The specific conversion processes are as follows.

3.3. Conic model conversion

First, the following new variables are defined:

$$\begin{cases} X_i = V^2 / \sqrt{2}, i = 1,2,..., n \\ Y_{ij} = V_i V_j \cos\theta_{ij}, j \in N(i) \\ Z_{ij} = V_i V_j \sin\theta_{ij} \end{cases} \tag{6}$$

V_i , V_i , θ_{ij} in the original model are replaced by X_i ,Y_{ij} ,Z_{ij}, respectively. Meanwhile, the formulas (2), (3), (4), (5) are converted into formulas (7), (8), (9), (10) , respectively.

$$\max \sum_{i=1}^{D} \left[\left| \sqrt{2} G_{ii} X_i + \sum_{j \in N(i)} \left(G_{ij} Y_{ij} + Bi_j Z_{ij} \right) \right| \right] \tag{7}$$

$$\begin{cases} P_{i\min} \le P_i = \sqrt{2} G_{ii} X_{\mathrm{i}}^{\ 2} + \sum_{j \in N(i)} \left(G_{ij} Y_{ij} + B_{ij} Z_{ij} \right) \le P_{imax} \\ Q_{i\min} \le Q_i = -\sqrt{2} B_{ii} X_{\mathrm{i}}^{\ 2} - \sum_{j \in N(i)} \left(B_{ij} Y_{ij} - G_{ij} Z_{ij} \right) \le Q_{imax} \end{cases} \tag{8}$$

$$\frac{V_{i\min}^2}{\sqrt{2}} \le X_i \le \frac{V_{i\max}^2}{\sqrt{2}} \tag{9}$$

$$I_{ij}^2 = \sqrt{2}A_{ij}X_i + \sqrt{2}B_{ij}X_i - 2C_{ij}Y_{ij} + 2D_{ij}Z_{ij} \le I_{ij\max}^2 \tag{10}$$

The model is based on the maximum supply capacity of load nodes, and it cannot calculate the generator node with load. If there is a generator node *i* with load, this paper will add a virtual node to separate the generator node and the load node. The node *i* will be divided into the generator node i_G and the load node i_L. The sketch diagram is shown in Fig. 3.

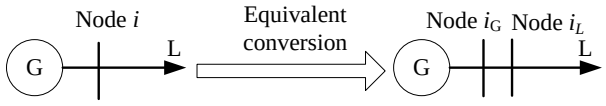

Fig. 3 Sketch map of generator virtual node

3.4. Adjustment of subareas boundaries

The boundaries between each subarea are power sources or tie-lines, and there is a mutual power supply among the subareas. In order to calculate the TSC value of each subarea independently, the boundaries of subareas need to be handled as follows.

1) If the boundaries of subareas are the tie-lines, the lines will be divided into the load bus i_L and generator bus i_G according to the active power flow direction. The bus i_L is equivalent to load for bus *i*, and the bus j_G is equivalent to source for bus *j*. The active power values of node *i* and node *j are* equal. This procedure can be sketched as Fig. 4.

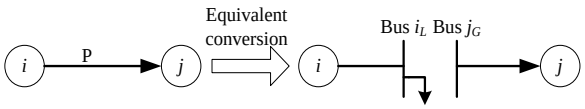

Fig. 4 Sketch of line virtual node

In order to find the TSC of the subarea where the node *j* is located, the maximum power output of virtual generator bus P_{jG} is calculated as

$$P_{jG} = P_{Li\max} - 1.1P_{i\max} \tag{11}$$

In the model, P_{Limax} is the maximum power supply that the bus *i* can obtain, and P_{imax} is the maximum load value of node *i*. The term 1.1 P_{imax} indicates that 10 percent of the load margin should be maintained to ensure the normal operation of the power system.

2) Consider the second case that the subareas boundaries are power sources. For a practical power system, the maximum power supply of the power source should be allocated in each subarea according to its power supply range. For the IEEE 118 bus test system, if the power source supplies power to multiple subareas, the maximum power supply of the power source is allocated according to the load ratio of each subarea.

4. Security indexes

In this paper, the security indexes of power system are based on the system structure, the TSC value and load factors. Several indexes are proposed in this paper to quantitatively evaluate the power system over-limits, load loss accidents and safety status, respectively.

4.1. Safety margin analysis

In the planning and operation of power systems, one of the most important principles is that the power system does not suffer from excessive load. Therefore, the safety margin (SM) is an important index of the security of power systems.

$$SM = \frac{TSC - \sum P_i}{\sum P_i} \tag{12}$$

where $\sum P_i$ is the sum of all loads at normal operation states. The SM value can reflect the overall security of the power system. Larger SM value shows that the system can withstand greater load increment or fluctuation.

4.2. Average system disequilibrium

The SM value can reflect the overall security of the power system, but this index cannot reflect the influence of partial security. Hence, SM value analysis is not a sufficient analysis of the security of power system. The load distribution equilibrium degree is an important factor to the partial security of power system. Therefore, the paper proposes the "average system disequilibrium" (ASD) index to reflect the partial security of the power system.

First, load rates are defined as follows:

μ_i is the load rate of each load node:

$$\mu_i = P_i / P_{i\max}, i = 1,2,..., D \tag{13}$$

where P_i is the load value at node *i*, and P_{imax} is the maximum power of load node *i*.

f_i is the load rate of transmission line *i*:

$$f_i = L_i / L_{i\max}, i = 1,2,..., D \tag{14}$$

where L_i is the actual transmitted power of line *i*, and L_{imax} is the maximum power of line *i*.

The formula of ASD is

$$ASD = \frac{1}{n}\left[\sum_{i=1}^{n}\left(k_i\mu_i - \frac{\sum_{1}^{n}\mu_i}{n}\right)^2 + \sum_{i=1}^{m}\left(k_i f_i - \frac{\sum_{1}^{m} f_i}{m}\right)^2\right] \tag{15}$$

where k_i is the important degree of load node (line) *i*. For a general load node (line), *k* is set to be 1, and for an important load node (line) *k* is set to a value larger than 1. The specific value of *k* is based on the practical situation.

At the same load level, the smaller the ASD value is, the higher security level of power system is.

4.3. Comprehensive safety analysis

Considering the influence of the overall security and the partial security on the security level of a power system, the comprehensive safety index (CSI) is proposed as follows. The CSI value refers to the ratio of the SM and ASD. This index is used to quantitatively reflect the comprehensive security of power systems.

$$CSI = \frac{SM}{1 + ASD} \tag{16}$$

The CSI is composed by the SM and ASD. The indexes of SM and ASD reflect the security level of the power system from different perspectives. The SM characterizes the overall security level of the power system, and ASD indicates partial security of the power system.

5. The security levels classification of power system

In order to describe the specific security status of power system, which will provide a benchmark to improve power system security, it is necessary to classify the security levels of power system.

The flowchart of the security level classification method is given as Fig. 5.

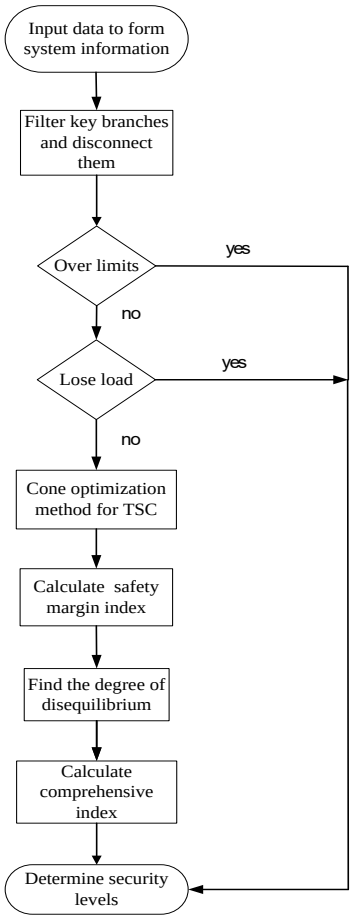

Fig. 5 Flowchart of the security level classification method

5.1. Principles

Since the security of the power system is influenced by both power system structure and its operation status, the security levels of the power system are classified based on its structure and operation status. The *N-k* contingency analysis fully considers the influence of these two security factors. Therefore, the security levels of the power system are assessed through *N-k* contingency analysis in this paper. If the power system does not meet the *N-k* contingency analysis, then *N-k*+1 contingency analysis is performed, and so on. If the power system does not meet the *N*-1 contingency requirement, the system will be classified as insecure.

5.2. Loss rate of load and over limits analysis

When the power system does not satisfy the *N*-1 contingency requirement, its security level is poor. If the load fluctuates suddenly, there may be some accidents in the power system due to poor security level. In order to reflect these accidents, this paper defines the loss rate of load index (LRL) and threshold crossing index (TC).

The LRL index is used to describe the severity of the load loss.

$$LRL = \frac{P_{loss}}{\sum_{i=1}^{n} P_i} \tag{17}$$

where P_{loss} is the load loss of the power system.

The TC is defined to characterize the risk of exceeding the capacity limit.

$$TC = \sum_{l=1}^{m} \omega_l \left(p_l^{\,*} / p_{l\max} \right)^2 \tag{18}$$

where m is the number of overloaded lines, $p_l^{\,*}$ is the active power flow of the overloaded lines, $p_{l\max}$ is the maximum capacity of the branch l, and ω_l is the weight of branch l. ω_l is determined by the magnitude of the load carried by the branch.

5.3. Security classification

The security levels are classified by threshold values. In historical studies, the thresholds of power system security levels are subjectively set, which cannot explain the practical significance of thresholds. In this paper, the security level thresholds (LT) are defined under the premise that the power system can meet *N-k* contingencies. The following threshold values are defined:

$$\begin{cases} LT1 = \dfrac{1.1(1+\alpha)^2 \sum_{i=1}^{n} p_{i\max} - \sum_{i=1}^{n} p_i}{\sum_{i=1}^{n} p_i} \\ LT2 = \dfrac{1.1P_{\max} - \sum_{i=1}^{n} p_i}{\sum_{i=1}^{n} p_i} \end{cases} \tag{19}$$

where $P_{\max}$ is the historical maximum load of the power system, p_{imax} is the historical maximum load of node i, and α is the annual load growth rate of the power system.

According to the values of LRL, TC and CSI, power systems are classified into five security levels.

Level I: CSI>LT1

It indicates that the power system can operate stably at a high security level, and it can withstand larger load fluctuations.

Level II: LT2<CSI<LT1

It shows that the power system can operate normally, and the power system can withstand certain extent of fluctuations.

Level III : 0<CSI<LT2

In this case, the power system can withstand a little load fluctuation, and the value of the real-time load should be adjusted to avoid accidents.

Level IV: TC>0

In this case, although the power system does not lose load, there is a risk of exceeding the relevant capacity limits. The greater the TC value is, the higher the risk of overload is.

Level V: LRL>0

It indicates that the power system would lose load when the *N*-1 contingency test is carried out. The power

supply-demand equilibrium cannot be achieved with load loss.

According to above method, this paper chooses 3 as the maximum value of *k* in the *N*-*k* contingency analysis. Therefore the security levels are sorted from high to low as follows:

1) The power system can withstand the *N*-3 contingencies.

2) The power system can withstand the *N*-2 contingencies.

3) The power system can withstand the *N*-1 contingency.

4) The power system has accidents of exceeding the limits under *N*-1 contingency.

5) The power system has accidents of lose load under *N*-1 contingency.

6) The security of a power system depends to a certain extent on the worst part.Therefore, when the two power system have the same security level, the power grid with the poorer area is less security.

6. Case studies

6.1. A practical power system

In this paper, a practical power system in China is selected for the simulation test. The power system has 6 transformer substations with the voltage level 220kV, 3 power plants, 20 transformer substations and 70 transmission lines with the voltage level 110kV. The transformer substations with 220kV and power plants are the sources of the transformer substations with 110kV. The system is shown as Fig. 6, where the rectangles represent the 220kV transformer substations and the circles represent the 110kV transformer substations.

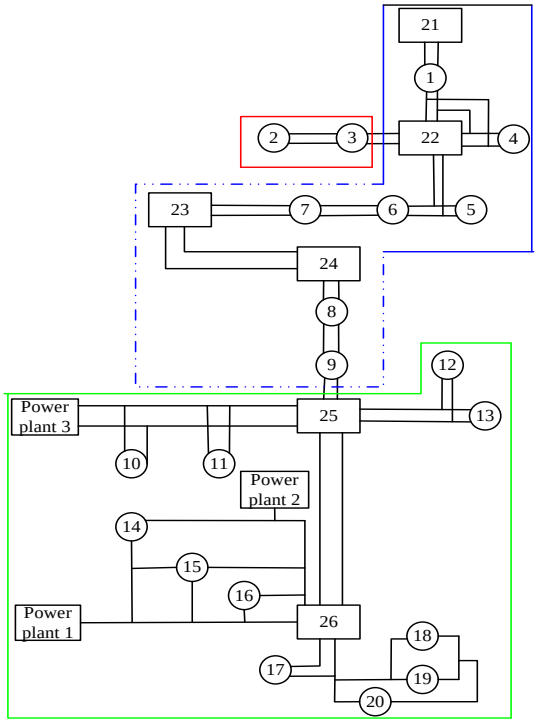

Fig. 6 A practical power system

6.2. Simulation results and analysis

Through the analysis of the power system structure and load condition, the 1, 4, 5, 6, 7, 8, 9 transformer substations can meet the *N*-2 contingencies, and the rest of 110kV transformer substations can meet the *N*-1 contingency. The power system is divided into three subareas based on the partitioning principles. The results are shown in Table 1.

Table 1 Power system partitioning results

subarea I	1, 4, 5, 6,7,8,9
subarea II	10-20
subarea III	2, 3

The TSC is obtained by filtering the expected faults and cone programming method. Combined with the load condition of each subarea, the SLC simulation results are shown in Fig. 7.

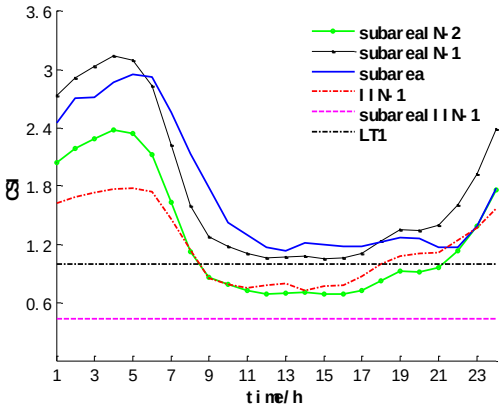

Fig. A

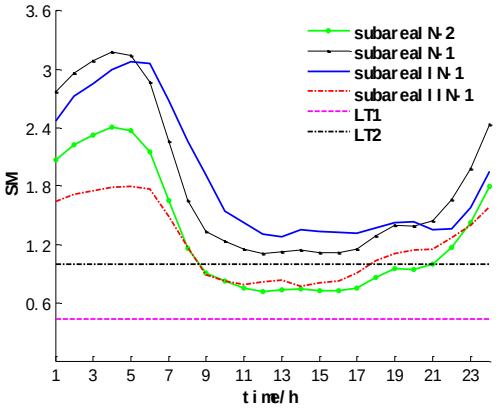

Fig. B

Fig. 7 SLC simulation results

Fig. A represents the comprehensive security level, which is obtained based on CSI. Fig. B represents the security level of safety margin, it is calculated from SM. The CSI value is lower than the SM value due to the ASD. Fig.8 represents the system disequilibrium degree that comes from ASD.

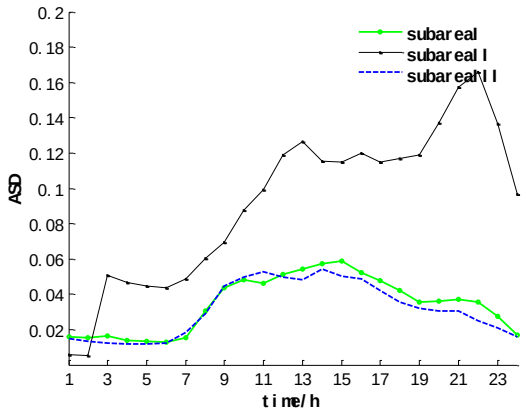

Fig. 8 system disequilibrium degree

Because the computation in each subarea is parallel computing, the maximum simulation time in the three subareas is the actual time used. The final simulation time of the practical system is 0.31s as shown in table 2, but the simulation time of the whole system is 0.58s. Therefore the computational time is reduced significantly.

Table 2 Simulation time

Region	Simulation time
whole system	0.58s
subarea I	0.28s
subarea II	0.31s
subarea III	0.25s

According to historical load condition and expected load growth rate of the power system, the threshold values of LT1 and LT2 are set as 1.05 and 0.46 respectively.

The following results can be obtained from the figures:

The CSI values of subarea I under *N*-1 contingency are above 1.05 in the whole day, and the security grade is level I. However the CSI values are decreased under *N*-2 contingencies. In the period of 8:00-21:00, CSI values are lower than 1.05 but higher than 0.46, and the security grade is level II. In the period of the 21:00-8:00, the CSI values are higher than 1.05, the security grade is level I. As for subarea II, the CSI values are higher than 1.05 in the whole day, the security grade is level I. For subarea III, in the period of 8:00-18:00 the security grade is level II, while in 18:00-8:00 it is level I. The security levels in the three subareas are significantly lower during the daytime than those at night. The reason is that the data used are those in the summer period in which electricity consumption in the daytime is much higher than the night.

In terms of operation status, the SM value of subarea II is the highest, its average margin is 1.89, the SM value is still over 1.28 even in peak load time. However, the system equilibrium degree of subarea II is obviously worse than other subareas. Its average system disequilibrium level is 0.092, and the highest value is up to 0.166. Hence, the load distribution of subarea II is uneven, the reason is that the subarea II has several main transformers with light load. The CSI values of subarea II are obviously lower than the SM value due to the high ASD value. The average CSI value is 1.75, and CSI is 1.13 at peak load time. As for subarea I, the average SM value is 1.83. Its load distribution is relatively balanced, the ASD value is only 0.034. Therefore, the CSI value is not much lower than the SM value, the average value of CSI is 1.78. The load distribution in subarea III is balanced, the ASD value is only 0.031. However, the load is heavy in this subarea. Its average SM value is only 0.76 at the peak load time, and the CSI value is only 0.72. Hence, the power system security level in subarea III is rather low. In terms of power system structure, the power system of subarea I can withstand *N*-2 contingencies, its security is the highest. The system of subarea III cannot meet the *N*-2 contingency, but the transformer substations are all double circuit connection, its structure security is high. As for the power system of subarea II, most of the substations are single line connection, its structure security is relatively poor.

Combined with the analysis of practical economic development, subarea I is located in the central business area of a city, and the load in this area is heavy. It will cause great economic loss once breakdown occurs, so the SM value and power system structure of subarea I are relatively high. Its overall security level is the highest in the three subareas, which has the security grade level II under *N*-2 contingencies. The subarea II is located in the suburbs, the load rate is relatively low, so its SM value is the highest. However, its power system structure is relatively simple, and cannot meet the *N*-2 contingencies. Thus, its overall security is lower than subarea I, and its security grade is level I under *N*-1 contingency. As for subarea III, its margin of safety load is low and is unable to withstand heavy load fluctuations. Its overall security is the worst with security grade level II under *N*-1 contingency. The power system needs expansion and reconstruction to increase operational security.

6.3. The IEEE 118-bus test system

As some nodes of the IEEE 118-bus test system have generator nodes with load, this paper will increase the virtual nodes to separate generator nodes and load nodes as Fig. 3.

In this paper, the IEEE 118-bus test system is divided into four kinds of subareas based on *N*-3, *N*-2, *N*-1 contingency and those which cannot withstand *N*-1 contingency. The isolated nodes are incorporated into the neighborhood according to the coupling relation between nodes.

The load nodes that satisfy the *N*-3 contingencies are separated into three subareas, the results is shown in Table 3.

Table 3 Subareas satisfying *N*-3 contingency

subarea 1	8, 11, 12, 15, 17, 19, 23, 24, 27, 31, 32, 18, 113（18 and 113 are incorporated from the isolated nodes which satisfied the *N*-2 contingency）
subarea 2	34, 40, 42, 46, 49, 54, 55, 56, 59, 62, 66, 70, 75, 77, 80, 60（60 is incorporated from the isolated nodes which satisfied the *N*-2 contingency）
subarea 3	85, 92, 94, 96, 100, 103, 104, 105, 110,90,91（90 and 91 are incorporated from the isolated nodes which satisfied the *N*-2 contingency）

The load nodes that satisfy the *N*-2 contingencies are separated into three subareas, the results is shown in Table 4.

Table 4 Subareas satisfying *N*-2 contingency

subarea 4	1, 3, 4, 6
subarea 5	36, 38, 45, 47, 51, 72, 74, 76, 82
subarea 6	99, 106, 107

The load nodes that satisfy the *N*-1 contingency are separated into three subareas, the results is shown in Table 5.

Table 5 Subareas satisfying *N*-1 contingency

subarea 7	2, 7, 13, 14, 16, 20, 21, 22, 28, 29, 33, 114, 115
subarea 8	35, 39, 41, 43, 44, 48, 50, 52, 53, 57, 58, 67, 73, 78, 79
subarea 9	84, 86, 88, 93, 95, 97, 98, 101, 102,108, 109, 112, 118, 116, 117（116 and 117 are incorporated from the isolated nodes which can not satisfied the *N*-1 contingency）

Since the IEEE 118-bus test system does not have historical load data, the LT values of security are tentatively scheduled for 1 and 0.6.

The simulation results show that the whole system is in a high security level under the normal operation of the system. The CSI values are larger than 1 except for subarea 9 of 0.962. Among them, the subarea 2 has the highest security level, and the average CSI value is 1.24. In the case of *N*-1 contingency, only subarea 2 and subarea 3 have CSI values larger than 1. When considering the *N*-2 and *N*-3 contingencies, the CSI values of all the subareas are less than 1. It is obvious that the contingencies of the power system have great influence on the security of power system.

The subareas security levels from high to low are ranked as follows: The subarea 2, 3 are in level II, and subarea 1 is in level III under *N*-3 contingencies. Subarea 6 and subarea 5 are in level II, subarea 4 in level III under *N*-2 contingencies. Subarea 3, 2 are in level II, and subarea 1 in level III under *N*-1 contingency.

When considering *N*-3, *N*-2 and *N*-1 contingency respectively, subarea 2 has the highest security level. The reason is that there are many generators in this area, and they have great mutual support ability due to the complex and close connection of the nodes. Hence, the system of subarea 2 can withstand large load fluctuations. The analysis of results also shows that if the subareas can only meet the N-1 contingency, their security levels are obviously poor. Hence, the power system structure has a great impact on security levels. In addition, when the contingencies occur in the power system, the system equilibrium degree will be worse. The reason is that the safety load margins of the load nodes near the fault position drop significantly. Besides, the simpler the power system structure is, the greater the system disequilibrium degree will be caused by the faults. To sum up, the security level of the power system is affected by its structure and the operation conditions, which verify the point of this paper.

7. Conclusions

In view of the deficiency of the traditional methods for security classification of power systems, this paper proposes a method for classifying the security levels based on the operation and network topology security. Firstly, the power system is divided into several subareas based on *N-k* contingencies, and this division can avoid the dimension disaster in the computation for large power systems. Secondly, the method of cone programming is used to obtain the TSC of each subarea, which greatly improves the computing speed. Then the security level of each subarea is quantitatively calculated based on the CSI and LT. The CSI fully considers the factors of power system operation and grid structure, and the LT is selected based on historical load data and future development plans. Finally, this security level classification method is applied to simulate and analyze a practical power system and the IEEE 118 bus test system. The rationality and feasibility of the proposed method are verified according to the simulations.

Acknowledgements

This work is financially supported by the National Natural Science Foundation of Hebei Province (No. F2016203507); and the National Natural Science Foundation of China (No. 61374098).

References

[1] Sun, Y,. Li, Z,. Wu, M.: 'The research on the cost compensation mechanism of the electric ancillary service under the new electricity reform'. Proc. int. Conf. Green Energy and Applications, Singapore, Mar.2017, pp. 74 - 79

[2] Xiang, Y., Ding, Z., Zhang, Y., et al.: 'Power System Reliability Evaluation Considering Load Redistribution Attacks', IEEE TRANSACTIONS ON SMART power system, 2017, 8(2), pp. 889-901

[3] Salloum, A., Al-Abdullah, Y. M., Vittal, V., et al.: 'Impacts of Constraint Relaxations on Power System Operational Security', IEEE Power and Energy Technology Systems, 2016, 3(2), pp. 99-108

[4] Qin, W,. Song, J,. Han, X,. Wang, P.: 'Operational reliability assessment of power systems based on bus voltage', *IET Gener. Transm. Distrib*, 2015, **9** (5), pp. 475-482

[5] Preece, R., Milanovic, J. V.: 'Risk-based small-disturbance security assessment of power systems', *IEEE Trans. Power Deliv.*, 2014, **30** (2), pp.590-598

[6] Bompard, E., Napoli, R., Xue, F.: 'Extended topological approach for the assessment of structural vulnerability in transmission networks', *IET Gener. Transm. Distrib*, 2010, **4** (6), pp. 716-724

[7] Doan, D.: 'Equipment Testing Safety', IEEE Industry Applications Magazine. 2017, 23, (4), pp. 6-7

[8] Srivani, J., Swarup, K. S.: 'Power system static security assessment and evaluation using external system equivalents', *Int. J. Elec. Power*, 2008, **30** (2), pp. 83-92

[9] Kalyani, S.: 'Pattern analysis and classification for security evaluation in power networks', *Int. J. Elec. Power*, 2013, 44 (1), pp. 547-560

[10] Lai, Y,. Chen, Y.: 'Decomposition Algorithm for the Dynamic Reactive Power Optimization of Large-Scale power system', Power System Technology, 2011, 5, (5) , pp. 37-41

[11] Yang, Y ., Guan, X ., Zhai, Q.: 'Fast power system Security Assessment With $N-k$ contingencies', IEEE Transactions on Power Systems, 2017, 32, (3), pp. 2193 - 2203

[12] Vu, T. L., Turitsyn, K.: 'A Framework for Robust Assessment of power system Stability and Resiliency', IEEE Transactions on Automatic Control. 2017, 62, (3) pp. 1165 - 1177

[13] Deng, S., Yue, D., Fu, X., Zhou, A.: 'Security risk assessment of cyber physical power system based on roughset and gene expression programming', IEEE/CAA Journal of Automatica Sinica, 2015, 2, (4), pp: 431 - 439

[14] Yan, W.,Gao, F.,Wang, F., et a1.: 'An optimal network partitioning algorithm for reactive power and voltage control considering subareaal reactive power margin', Power System Technology, 2015,39(2), pp. 61-66

[15] Jiang, T,. Bai, L,. Yuan, H,. et a1.: 'QV interaction evaluation and pilot voltage-reactive power coupling area partitioning in bulk power

systems', IET Science, Measurement & Technology, 2017, 11, (3) pp. 270-278
[16] I Kamwa, AK Pradhan, G Joos, SR Samantaray.: 'Fuzzy partitioning of a real power system for dynamic vulnerability assessment', IEEE Transactions on Power Systems, 2009, 24, (3), pp. 1356-1365
[17] I Kamwa, AK Pradhan, G Joos.: 'Automatic segmentation of large power systems into fuzzy coherent areas for dynamic vulnerability assessment', IEEE Transactions on Power Systems, 2007, 22, (4), pp. 1974-1985
[18] Jingjing, Z., We,i W., Chengshan, W.: 'Distributed transfer capability computation of electric power system based on decomposed system network', Proceedings of the CSEE, 2008, 28, (7) pp. 1-6
[19] Ma, L,. Jia, B,. Cao, L.: 'Research on Security Classification of Transmission Network Considering Static Security and Real-Time Power Supply Capability', Transactions of China Electrotechnical Society, 2014, 29(6).pp. 229-237
[20] Xiao, J., Liu, S., Li, Z., Li, F.: 'Loadability formulation and calculation for interconnected distribution systems considering N-1 security', *Int. J. Elec. Power*, 2016, 77, pp. 70-76
[21] Li, W,. Qi, S,. Mou, X,.et al.: 'A Recursive Network Partitioning Method for Reactive Power/Voltage Control Based on the Analysis of Node Coupling Relationships', Proceedings of the CSEE, 2014, 34, (31), pp.5625-5632
[22] Cai, J., Bai, T., Hou, Z.: ' Improvement of contingency ranking method for power system on-line security analysis', Automation of Electric Power Systems, 2000, 24, (19), pp. 25-28
[23] Zhou, H., Liu, D., Wu, Z, et al.: 'Power system security alarm assessment index and its application', Automation of Electric Power Systems, 2007, 31, (20) , pp. 45-48
[24] Xiao, J., Li, F., Gu, W.: 'Total supply capability and its extended indices for distribution systems: definition, model calculation and applications', *IET Gener. Transm. Distrib.*, 2011, **5** (8), pp. 869-876
[25] Jabr, R. A. Singh, R., Pal, B. C.: 'Minimum loss network reconfiguration using mixed-integer convex programming', IEEE Transactions on Power Systems, 2012, 27, (2), pp. 1106-1115
[26] Lu, Z., He, L., Zhang, D,. Zhao, B,. et al.: 'A Security Level Classification Method for Power Systems under N-1 Contingency', Energies, 2017, 10, (12), pp. 2055-2072